**Preprints of the 19th World Congress**
**The International Federation of Automatic Control**
**Cape Town, South Africa. August 24-29, 2014**

# $\mathcal{H}_\infty$ Synthesis Method for Control of Non-linear Flexible Joint Models ⋆

**Patrik Axelsson,** * **Goele Pipeleers,** ** **Anders Helmersson,** * **Mikael Norrlöf** *,***

* *Division of Automatic Control, Department of Electrical Engineering, Linköping University, SE-581 83 Linköping, Sweden (e-mail: {axelsson, andersh, mino}@isy.liu.se).*
** *Department of Mechanical Engineering, Katholieke Universiteit Leuven, Celestijnenlaan 300B, B-3001 Heverlee, Belgium (e-mail: goele.pipeleers@mech.kuleuven.be).*
*** *ABB AB – Robotics SE-721 68 Västerås, Sweden.*

**Abstract:** An $\mathcal{H}_\infty$ synthesis method for control of a flexible joint, with non-linear spring characteristic, is proposed. The first step of the synthesis method is to extend the joint model with an uncertainty description of the stiffness parameter. In the second step, a non-linear optimisation problem, based on nominal performance and robust stability requirements, has to be solved. Using the Lyapunov shaping paradigm and a change of variables, the non-linear optimisation problem can be rewritten as a convex, yet conservative, LMI problem. The method is motivated by the assumption that the joint operates in a specific stiffness region of the non-linear spring most of the time, hence the performance requirements are only valid in that region. However, the controller must stabilise the system in all stiffness regions. The method is validated in simulations on a non-linear flexible joint model originating from an industrial robot.

Keywords: Mechanical systems, Flexible, Robust, H-infinity Control

## 1. INTRODUCTION

The demand and the requirements for high precision control in electro mechanical systems have been increasing over time. At the same time cost reduction and more developed mechanical design criteria, with lower margins in the design, reduces the size of the components involved. One such example is the speed reducers used in many electro mechanical systems where the size and cost have become increasingly important. The harmonic drive, sometimes referred to as “strain-wave gearing”, is a very common example of a gear type that can deliver high gear reduction ratio in a small device [Tuttle and Seering, 1996]. Characteristic to compact gear boxes, such as harmonic drives, are that they have a relatively small backlash, a highly non-linear friction behaviour, and in addition a very non-linear stiffness [Tjahjowidodo et al., 2006]. One typical application of electromechanical systems, where harmonic drive gearboxes are used, is in industrial robots where the motivation for the work presented in this paper also comes from. In this paper the control design for the electromechanical system, motor-gearbox joint, hereafter referred to as the *flexible joint system*, is considered. In general, robots are strongly coupled multivariate systems with non-linear dynamics and in previous research on control of robots linear spring stiffness has been considered, see e.g. Sage et al. [1999] and the references therein. When the speed reducers are of harmonic drive type, linear models are however not sufficient for the control as will be shown in the paper. Several non-linear models of the gearbox have been presented in the literature, see Tuttle and Seering [1996], Tjahjowidodo et al. [2006], Ruderman and Bertram [2012] among others.

⋆ This work was supported by the Vinnova Excellence Center LINK-SIC and by the Excellence Center at Linköping-Lund in Information Technology, ELLIIT.

What characterises the $\mathcal{H}_\infty$-controller synthesis method presented in this work is that it can facilitate in designing a controller which gives performance in one region of parameter values, while for another region the performance requirement is lower and only stability is sufficient. The proposed method is motivated by the fact that the flexible joint operates in specific regions most of the time. For example, a joint which is affected by gravity operates most of the time in the high stiffness region, hence it is more important to have a controller with good performance in the high stiffness region. However, the controller must stabilise the system in all stiffness regions.

This paper is organised as follows. Section 2 presents the problem and how it will be solved and the proposed method is outlined in Section 3. In Section 4, the non-linear joint model used to test the proposed method is presented. The design of the controller and the results are given in Sections 5 and 6. Finally, Section 7 concludes the paper.

## 2. PROBLEM FORMULATION

The problem is to design a linear $\mathcal{H}_\infty$-controller that can stabilise a non-linear flexible joint model, for example a motor-harmonic drive-joint system, using only the primary position, the motor position $q_m$. There are a number of non-linearities that characterise the gearbox in the flexible joint. Here, the spring stiffness of the joint is considered and it is described by the function $\tau_s(\Delta_q)$, where $\Delta_q = q_m - q_a$ is the deflection between the motor position $q_m$ and the secondary position, the arm position $q_a$. The non-linear spring is characterised by a low stiffness for

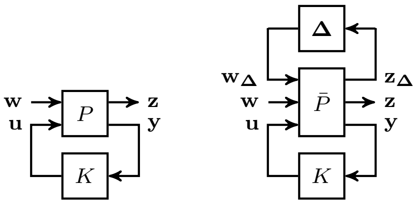


(a) (b)

Fig. 1. Closed-loop system from $\mathbf{w}$ to $\mathbf{z}$, without and with an uncertainty description in (a) and (b) respectively.

small deflections and a high stiffness for large deflections, which is typical for compact gear boxes, such as harmonic drive [Tuttle and Seering, 1996, Ruderman and Bertram, 2012]. Linearising the stiffness function would give a linear expression $k \cdot (q_m - q_a)$, where the gain $k$ depends on the deflection $q_m - q_a$ of the joint. The lowest and maximal values of $k$ are $k^{\text{low}}$ and $k^{\text{high}}$, respectively. The complete model and an explicit expression for $\tau_s(\Delta_q)$ are presented in Section 4.

Control of non-linear systems using linear $\mathcal{H}_\infty$-methods is usually done by first linearising the model in several operating points, e.g. gain scheduling techniques, or using exact linearisation. Gain scheduling requires to know the operating point of the spring and exact linearisation requires the full state vector, hence only the motor position is not enough to measure. A common solution is to introduce an observer for estimating the state vector. However, it is not certain that the estimated state vector is accurate enough to use due to model errors and disturbances. The estimation problem has been investigated in e.g. Axelsson et al. [2012], Chen and Tomizuka [2013].

Instead, the problem considered in this paper is managed using an uncertainty description of the stiffness parameter $k$ to obtain a controller over the whole interval for $k$. In general, the interval has to be relative short in order to obtain a controller using regular methods. The reason for this is that the methods try to be both robustly stable and have robust performance over the whole interval. The uncertainty description of the linearised spring stiffness can give a long interval of the parameter $k$ that has to be covered. Instead of having a controller that satisfies the requirements of both robust stability and performance over the whole interval, the aim is to find a controller that is stable for all values of $k$ but only satisfies the performance requirements in the high stiffness region. The reason for this is that in practice, the joint operates only in the high stiffness region most of the time, e.g. an industrial manipulator affected by the gravity force. In reality as low as zero stiffness must be handled due to backlash, but that is omitted here.

## 3. PROPOSED $\mathcal{H}_\infty$ SYNTHESIS METHOD

This section presents the proposed $\mathcal{H}_\infty$ synthesis method. First, the uncertainty description is given. After that, the requirement for nominal stability and performance together with robust stability is discussed, and the final optimisation problem is presented.

### 3.1 Uncertainty Description

Let $k$ be modelled as an uncertainty according to

$$k(\delta) = k + \bar{k}\delta, \tag{1a}$$

$$k = \alpha k^{\text{high}} + \beta k^{\text{low}}, \tag{1b}$$

$$\bar{k} = \alpha k^{\text{high}} - \beta k^{\text{low}}, \tag{1c}$$

where $\alpha$, $\beta$ are scaling parameters such that $\beta \leq \alpha$. The uncertain parameter $\delta$ is contained in $\boldsymbol{\delta} = [-1\ 1] \subset \mathbb{R}$ and may change arbitrarily fast. For $\delta = \pm 1$ it holds that the stiffness parameter

$$k(\delta) \in \left[2\beta k^{\text{low}}\ \ 2\alpha k^{\text{high}}\right]. \tag{2}$$

Since the aim is to have a controller that has good performance in the high stiffness region, but only stable in the low stiffness region, it is desirably to have $k$ close to $k^{\text{high}}$ and the lower bound of $k(\delta)$ not larger than $k^{\text{low}}$.

The stiffness parameter enters only in the $A$-matrix of the linearised system and assume that the part containing $\delta$ is of rank one, then

$$\mathbf{A}(\delta) = \mathbf{A} + \mathbf{L}\delta\mathbf{R} \tag{3}$$

with $\mathbf{A} \in \mathbb{R}^{n_x \times n_x}$, $\mathbf{L} \in \mathbb{R}^{n_x,1}$ and $\mathbf{R} \in \mathbb{R}^{1,n_x}$. For the forthcoming calculations, it is important to have $\mathbf{L}$ and $\mathbf{R}$ as a column and row matrix, respectively. The augmented system in Figure 1(b) can now be constructed according to

$$\bar{P} = \left(\begin{array}{c|ccc} \mathbf{A} & \mathbf{L} & \mathbf{B_w} & \mathbf{B_u} \\ \hline \mathbf{R} & \mathbf{0} & \mathbf{0} & \mathbf{0} \\ \mathbf{C_z} & \mathbf{0} & \mathbf{D_{zw}} & \mathbf{D_{zu}} \\ \mathbf{C_y} & \mathbf{0} & \mathbf{D_{yw}} & \mathbf{0} \end{array}\right), \tag{4}$$

with $\boldsymbol{\Delta} = \delta$.

### 3.2 Nominal Stability and Performance

Let $P$ represent an LTI system, see Figure 1(a),

$$\dot{\mathbf{x}} = \mathbf{A}\mathbf{x} + \mathbf{B_w}\mathbf{w} + \mathbf{B_u}\mathbf{u}, \tag{5a}$$

$$\mathbf{z} = \mathbf{C_z}\mathbf{x} + \mathbf{D_{zw}}\mathbf{w} + \mathbf{D_{zu}}\mathbf{u}, \tag{5b}$$

$$\mathbf{y} = \mathbf{C_y}\mathbf{x} + \mathbf{D_{yw}}\mathbf{w}, \tag{5c}$$

where $\mathbf{x} \in \mathbb{R}^{n_x \times 1}$ is the state vector, $\mathbf{w} \in \mathbb{R}^{n_w \times 1}$ is the disturbance vector, $\mathbf{u} \in \mathbb{R}^{n_u \times 1}$ is the control signal, $\mathbf{y} \in \mathbb{R}^{n_y \times 1}$ is the measurement signal, and $\mathbf{z} \in \mathbb{R}^{n_z \times 1}$ is the output signal that reflects our specifications. The matrices in (5) has dimensions corresponding to the vectors $\mathbf{x}$, $\mathbf{w}$, $\mathbf{u}$, $\mathbf{y}$, and $\mathbf{z}$. Note that it is the nominal system, i.e., $\delta = 0$ that is used here. Let the controller $K$ in Figure 1(a) be given by

$$\dot{\mathbf{x}}_K = \mathbf{A}_K\mathbf{x}_K + \mathbf{B}_K\mathbf{y}, \tag{6a}$$

$$\mathbf{u} = \mathbf{C}_K\mathbf{x}_K + \mathbf{D}_K\mathbf{y}. \tag{6b}$$

Using the lower fractional transformation $F_l(P, K)$ gives the closed loop system from $w$ to $z$ according to

$$F_l(P,K) = \left(\begin{array}{c|c} \mathbf{A}_{CL} & \mathbf{B}_{CL} \\ \hline \mathbf{C}_{CL} & \mathbf{D}_{CL} \end{array}\right)$$

$$= \left(\begin{array}{cc|c} \mathbf{A} + \mathbf{B_u}\mathbf{D}_K\mathbf{C_y} & \mathbf{B_u}\mathbf{C}_K & \mathbf{B_w} + \mathbf{B_u}\mathbf{D}_K\mathbf{D_{yw}} \\ \mathbf{B}_K\mathbf{C_y} & \mathbf{A}_K & \mathbf{B}_K\mathbf{D_{yw}} \\ \hline \mathbf{C_z} + \mathbf{D_{zu}}\mathbf{D}_K\mathbf{C_y} & \mathbf{D_{zu}}\mathbf{C}_K & \mathbf{D_{zw}} + \mathbf{D_{zu}}\mathbf{D}_K\mathbf{D_{yw}} \end{array}\right) \tag{7}$$

From Gahinet and Apkarian [1994] it holds that the $\mathcal{H}_\infty$-norm of $F_l(P, K)$ is less than $\gamma$, i.e., $\|F_l(P,K)\|_\infty < \gamma$, and the closed loop system is stable, i.e., $\mathbf{A}_{CL}$ has all eigenvalues in the left half plane, if and only if there exists a positive definite matrix $\boldsymbol{\mathcal{P}}$ such that

$$\begin{pmatrix} \mathbf{A}_{CL}^{\mathsf{T}}\boldsymbol{\mathcal{P}} + \boldsymbol{\mathcal{P}}\mathbf{A}_{CL} & \boldsymbol{\mathcal{P}}\mathbf{B}_{CL} & \mathbf{C}_{CL}^{\mathsf{T}} \\ \mathbf{B}_{CL}^{\mathsf{T}}\boldsymbol{\mathcal{P}} & -\gamma\mathbf{I} & \mathbf{D}_{CL}^{\mathsf{T}} \\ \mathbf{C}_{CL} & \mathbf{D}_{CL} & -\gamma\mathbf{I} \end{pmatrix} \prec 0. \tag{8}$$

### *3.3 Robust Stability*

To guarantee robust stability of the uncertain system for arbitrarily fast changes in $\delta$, quadratic stability is enforced which is given by

$$\exists \boldsymbol{\mathcal{P}} \in \mathbb{S}^{n_x} : \boldsymbol{\mathcal{P}} \succ 0 \text{ and} \tag{9a}$$

$$\mathbf{A}(\delta)^{\mathsf{T}} \boldsymbol{\mathcal{P}} + \boldsymbol{\mathcal{P}} \mathbf{A}(\delta) \prec 0, \; \forall \delta \in \boldsymbol{\delta}. \tag{9b}$$

From Scherer [2006], the robust LMI (9b) holds if and only if there exist $p, q \in \mathbb{R}$ with $p > 0$ such that

$$\begin{pmatrix} \mathbf{I} & \mathbf{0} \\ \mathbf{A} & \mathbf{L} \end{pmatrix}^{\mathsf{T}} \begin{pmatrix} \mathbf{0} & \boldsymbol{\mathcal{P}} \\ \boldsymbol{\mathcal{P}} & \mathbf{0} \end{pmatrix} \begin{pmatrix} \mathbf{I} & \mathbf{0} \\ \mathbf{A} & \mathbf{L} \end{pmatrix} + \begin{pmatrix} \mathbf{0} & \mathbf{I} \\ \mathbf{R} & \mathbf{0} \end{pmatrix}^{\mathsf{T}} \begin{pmatrix} -p & iq \\ -iq & p \end{pmatrix} \begin{pmatrix} \mathbf{0} & \mathbf{I} \\ \mathbf{R} & \mathbf{0} \end{pmatrix} \prec 0 \tag{10}$$

Note that $p, q \in \mathbb{R}$ with $p > 0$ parametrize all multipliers that satisfy

$$\begin{pmatrix} \delta \\ 1 \end{pmatrix}^{\mathsf{T}} \begin{pmatrix} -p & iq \\ -iq & p \end{pmatrix} \begin{pmatrix} \delta \\ 1 \end{pmatrix} \geq 0, \; \forall \delta \in \boldsymbol{\delta}. \tag{11}$$

Since the negative definiteness of a Hermitian matrix implies that its real part is negative definite, $q = 0$ can be enforced in (10) without loss of generality. It follows from the fact that $\mathbf{L}$ and $\mathbf{R}$ are rank one matrices [1] . In addition, $p = 1$ can be enforced since the LMI is homogeneous in $\boldsymbol{\mathcal{P}}$ and $p$. By elaborating the left-hand side of (10) gives that (9) is equivalent to

$$\exists \boldsymbol{\mathcal{P}} \in \mathbb{S}^{n_x} : \boldsymbol{\mathcal{P}} \succ 0 \text{ and } \begin{pmatrix} \mathbf{A}^{\mathsf{T}} \boldsymbol{\mathcal{P}} + \boldsymbol{\mathcal{P}} \mathbf{A} + \mathbf{R}^{\mathsf{T}} \mathbf{R} & \boldsymbol{\mathcal{P}} \mathbf{L} \\ \mathbf{L}^{\mathsf{T}} \boldsymbol{\mathcal{P}} & -1 \end{pmatrix} \prec 0. \tag{12}$$

The last LMI in (12) can be rewritten, similar to what is given by (8), using the Schur complement, according to

$$\begin{pmatrix} \mathbf{A}^{\mathsf{T}} \boldsymbol{\mathcal{P}} + \boldsymbol{\mathcal{P}} \mathbf{A} & \boldsymbol{\mathcal{P}} \mathbf{L} & \mathbf{R}^{\mathsf{T}} \\ \mathbf{L}^{\mathsf{T}} \boldsymbol{\mathcal{P}} & -1 & 0 \\ \mathbf{R} & 0 & -1 \end{pmatrix} \prec 0. \tag{13}$$

The LMI in (12) can also be obtained using IQC-based robust stability analysis with frequency independent multipliers [Megretski and Rantzer, 1997], which guarantees stability for arbitrarily fast changes in $\delta$.

### *3.4 Controller Synthesis*

The controller is now obtained from the following optimisation problem

$$\underset{A_K, B_K, C_K, D_K}{\text{Minimise}} \quad \gamma \tag{14a}$$

$$\text{subject to} \quad \boldsymbol{\mathcal{P}} \succ 0 \tag{14b}$$

$$\begin{pmatrix} \mathbf{A}_{CL}^{\mathsf{T}} \boldsymbol{\mathcal{P}} + \boldsymbol{\mathcal{P}} \mathbf{A}_{CL} & \boldsymbol{\mathcal{P}} \mathbf{B}_{CL} & \mathbf{C}_{CL}^{\mathsf{T}} \\ \mathbf{B}_{CL}^{\mathsf{T}} \boldsymbol{\mathcal{P}} & -\gamma \mathbf{I} & \mathbf{D}_{CL}^{\mathsf{T}} \\ \mathbf{C}_{CL} & \mathbf{D}_{CL} & -\gamma \mathbf{I} \end{pmatrix} \prec 0 \tag{14c}$$

$$\begin{pmatrix} \mathbf{A}_{CL}^{\mathsf{T}} \boldsymbol{\mathcal{P}} + \boldsymbol{\mathcal{P}} \mathbf{A}_{CL} & \boldsymbol{\mathcal{P}} \mathbf{L}_{CL} & \mathbf{R}_{CL}^{\mathsf{T}} \\ \mathbf{L}_{CL}^{\mathsf{T}} \boldsymbol{\mathcal{P}} & -1 & 0 \\ \mathbf{R}_{CL} & 0 & -1 \end{pmatrix} \prec 0 \tag{14d}$$

where $\mathbf{L}_{CL}$ and $\mathbf{R}_{CL}$ are the matrices $\mathbf{L}$ and $\mathbf{R}$ augmented with zeros in order for the dimensions to satisfy the closed-loop state vector $\mathbf{x}_{CL} = \left(\mathbf{x}^{\mathsf{T}} \; \mathbf{x}_K^{\mathsf{T}}\right)^{\mathsf{T}}$.

The minimisation problem in (14) gives a conservative solution because of the same Lyapunov matrix $\boldsymbol{\mathcal{P}}$ is used in both (8) and (13). For the approach not to be conservative, different Lyapunov matrices should be used in (8) and (13). However, this multi-objective controller design is non-convex. To obtain a convex, yet conservative, approximation, the Lyapunov shaping paradigm, as introduced by Scherer et al. [1997], is used. Moreover, the minimisation problem in (14) is non-linear due to products of $\boldsymbol{\mathcal{P}}$ and the controller parameters $\mathbf{A}_K$, $\mathbf{B}_K$, $\mathbf{C}_K$, and $\mathbf{D}_K$. However, a change of variables [Scherer et al., 1997] makes the constraints linear and the resulting minimisation problem can be solved using LMI optimisation, e.g. using Yalmip [Löfberg, 2004].

[1] If $\operatorname{rank} \mathbf{L} = \operatorname{rank} \mathbf{R} = r$, than $q$ should be a $r \times r$ skew symmetric matrix and the involved computations are much more complex.

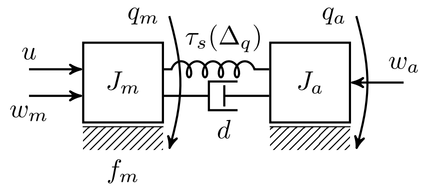


Fig. 2. A two-mass flexible joint model, where $J_m$ is the motor and $J_a$ the arm.

The optimisation problem (14) will be easier to solve the smaller the perturbation is. It can therefore be useful to introduce a scaling parameter $0 < \kappa \leq 1$ such that $\delta \in [-\kappa \; \kappa]$. Decreasing $\boldsymbol{\delta}$ to $[-\kappa \; \kappa]$ is equivalent to preserving $\boldsymbol{\delta} = [-1 \; 1]$ but rescaling $\mathbf{L}$, according to $\mathbf{L} \to \kappa \mathbf{L}$. The good thing is that it can still be possible to stabilise the system for $\delta \in [-1 \; 1]$ due to the conservatism of the proposed method. Note that $\kappa$ is a tuning parameter that affect the solution to (14). A too large value can make the problem impossible to solve whereas a too small value gives a controller that is not able to stabilise the non-linear system.

## 4. NON-LINEAR FLEXIBLE JOINT MODEL

The flexible joint model considered in this paper is of two-mass model type, see Figure 2, where $q_m$ is the motor position and $q_a$ the arm position. Here, both $q_m$ and $q_a$ are described on the motor side of the gearbox. Input to the system is the motor torque $u$, the motor disturbance $w_m$ and the arm disturbance $w_a$. The two masses are connected by a spring-damper pair, where the first mass corresponds to the motor and the second mass corresponds to the arm. The spring-damper pair is modelled by a linear damper, described by the parameter $d$, and the non-linear spring is described by the function $\tau_s(\Delta_q)$ which is a piecewise affine function with five segments, i.e.,

$$\tau_s(\Delta_q) = \begin{cases} k_{\text{low}} \Delta_q, & |\Delta_q| \leq \dfrac{\Psi}{4} \\ (k_{\text{low}} + m_k)\, \Delta_q - \operatorname{sign}(\Delta_q) \dfrac{m_k \Psi}{4}, & \dfrac{\Psi}{4} < |\Delta_q| \leq \dfrac{\Psi}{2} \\ (k_{\text{low}} + 2m_k)\, \Delta_q - \operatorname{sign}(\Delta_q) \dfrac{3m_k \Psi}{4}, & \dfrac{\Psi}{2} < |\Delta_q| \leq \dfrac{3\Psi}{4} \\ (k_{\text{low}} + 3m_k)\, \Delta_q - \operatorname{sign}(\Delta_q) \dfrac{3m_k \Psi}{2}, & \dfrac{3\Psi}{4} < |\Delta_q| \leq \Psi \\ k_{\text{high}} \Delta_q - \operatorname{sign}(\Delta_q) \dfrac{5m_k \Psi}{2}, & \Psi < |\Delta_q| \end{cases}$$

where $m_k = (k_{\text{high}} - k_{\text{low}})/4$, and $\Psi$ a model parameter describing the transition to the high stiffness region. Moreover, the friction torque is assumed to be linear, described

Table 1. Numerical values of the model parameters.

| $J_a$ | $J_m$ | $\Psi$ | $k_{\text{high}}$ | $k_{\text{low}}$ | $d$ | $f_m$ |
|---|---|---|---|---|---|---|
| 0.042 | 0.005 | $220\pi/60/180$ | 100 | 100/6 | 0.08 | 0.006 |

by the parameter $f_m$, and the input torque $u$ is limited to $\pm 20\,\text{Nm}$. The measurement of the system is the motor position $q_m$, and $q_a$ is the variable that is to be controlled. The model is a simplification of the experimental results achieved in, e.g. Tjahjowidodo et al. [2006], where the non-linear torsional stiffness also shows hysteresis behaviour.

The dynamical model of the flexible joint is given by

$$J_a\ddot{q}_a - \tau_s(\Delta_q) - d(\dot{q}_m - \dot{q}_a) = w_a, \tag{15a}$$

$$J_m\ddot{q}_m + \tau_s(\Delta_q) + d(\dot{q}_m - \dot{q}_a) + f_m\dot{q}_m = u + w_m, \tag{15b}$$

where the model parameters are presented in Table 1. Using a state vector $x$ according to

$$\mathbf{x} = \left(q_a \ q_m \ \dot{q}_a \ \dot{q}_m\right)^{\mathsf{T}}, \tag{16}$$

gives the non-linear state space model

$$\dot{\mathbf{x}} = \begin{pmatrix} \dot{q}_a \\ \dot{q}_m \\ \dfrac{1}{J_a}\left(\tau_s(\Delta_q) + d(\dot{q}_m - \dot{q}_a) + w_a\right) \\ \dfrac{1}{J_m}\left(u - \tau_s(\Delta_q) - d(\dot{q}_m - \dot{q}_a) - f_m\dot{q}_m + w_m\right) \end{pmatrix} \tag{17}$$

Linearising the non-linear flexible joint model (17) gives a linear state space model $\dot{\widetilde{\mathbf{x}}} = \widetilde{\mathbf{A}}\widetilde{\mathbf{x}} + \widetilde{\mathbf{B}}_{\mathbf{u}}\mathbf{u} + \widetilde{\mathbf{B}}_{\mathbf{w}}\mathbf{w}$, where $\mathbf{w} = \left(w_a \ w_m\right)^{\mathsf{T}}$ and

$$\widetilde{\mathbf{A}} = \begin{pmatrix} 0 & 0 & 1 & 0 \\ 0 & 0 & 0 & 1 \\ -\dfrac{k}{J_a} & \dfrac{k}{J_a} & -\dfrac{d}{J_a} & \dfrac{d}{J_a} \\ \dfrac{k}{J_m} & -\dfrac{k}{J_m} & \dfrac{d}{J_m} & -\dfrac{d+f_m}{J_m} \end{pmatrix}, \tag{18a}$$

$$\widetilde{\mathbf{B}}_{\mathbf{u}} = \begin{pmatrix} 0 \\ 0 \\ 0 \\ \dfrac{1}{J_m} \end{pmatrix}, \quad \widetilde{\mathbf{B}}_{\mathbf{w}} = \begin{pmatrix} 0 & 0 \\ 0 & 0 \\ \dfrac{1}{J_a} & 0 \\ 0 & \dfrac{1}{J_m} \end{pmatrix} \tag{18b}$$

$$\widetilde{\mathbf{C}} = \left(0 \ 1 \ 0 \ 0\right). \tag{18c}$$

Here, $k$ is the stiffness parameter given by (1b). The uncertainty description (1) gives

$$\widetilde{\mathbf{A}}(\delta) = \widetilde{\mathbf{A}} + \widetilde{\mathbf{L}}\delta\widetilde{\mathbf{R}}, \tag{19a}$$

$$\widetilde{\mathbf{L}} = \left(0 \ 0 \ \frac{\bar{k}}{J_a} \ -\frac{\bar{k}}{J_m}\right)^{\mathsf{T}}, \tag{19b}$$

$$\widetilde{\mathbf{R}} = \left(-1 \ 1 \ 0 \ 0\right). \tag{19c}$$

The notation $\widetilde{\ }$ indicates that the weighting functions in the system $P(s)$ is not included here. Section 5 presents the weighting functions and how they are included in the state space model to give the system $P(s)$ in (5).

## 5. CONTROLLER DESIGN

A common design method is to construct the system $P$ in (5) by augmenting the original system $\mathbf{y} = G(s)\mathbf{u}$ with the weights $W_{\mathbf{u}}(s)$, $W_S(s)$, and $W_T(s)$, such that the system $\mathbf{z} = F_l(P,K)\mathbf{w}$, depicted in Figure 1(a), can be written as

$$F_l(P,K) = \begin{pmatrix} W_{\mathbf{u}}(s)G_{\mathbf{wu}}(s) \\ -W_T(s)T(s) \\ W_S(s)S(s) \end{pmatrix}, \tag{20}$$

where $S(s) = (I + G(s)K(s))^{-1}$ is the sensitivity function, $T(s) = I - S(s)$ is the complementary sensitivity function, and $G_{\mathbf{wu}}(s) = -K(s)(I + G(s)K(s))^{-1}$ is the transfer function from $\mathbf{w}$ to $\mathbf{u}$. The $\mathcal{H}_\infty$-controller is obtained by minimising the $\mathcal{H}_\infty$-norm of the system $F_l(P,K)$, i.e., minimise $\gamma$ such that $\|F_l(P,K)\|_\infty < \gamma$. Using (20) gives

$$|W_{\mathbf{u}}(i\omega)G_{\mathbf{wu}}(i\omega)| < \gamma, \ \forall\omega, \tag{21a}$$

$$|W_T(i\omega)T(i\omega)| < \gamma, \ \forall\omega, \tag{21b}$$

$$|W_S(i\omega)S(i\omega)| < \gamma, \ \forall\omega. \tag{21c}$$

The transfer functions $G_{\mathbf{wu}}(s)$, $S(s)$, and $T(s)$ can now be shaped to satisfy the requirements by choosing the weights $W_{\mathbf{u}}(s)$, $W_S(s)$, and $W_T(s)$. In general this is a quite difficult task. See e.g. Skogestad and Postletwaite [2005], Zhou et al. [1996] for details.

The mixed-$\mathcal{H}_\infty$ controller design [`mixedHinfsyn`, 2013, Zavari et al., 2012] is a modification of the standard $\mathcal{H}_\infty$ design method. Instead of choosing the weights in (20) such that the norm of all weighted transfer functions satisfies (21), the modified method divides the problem into design constraints and design objectives. The controller can now be found as the solution to

$$\underset{K(s)}{\text{Minimise}} \quad \gamma \tag{22a}$$

$$\text{subject to} \quad \|W_P S\| < \gamma \tag{22b}$$

$$\|M_S S\| < 1 \tag{22c}$$

$$\|W_{\mathbf{u}} G_{\mathbf{wu}}\| < 1 \tag{22d}$$

$$\|W_T T\| < 1 \tag{22e}$$

where $\gamma$ not necessarily has to be close to 1. The LMI in (8) can be modified to fit into the optimisation problem (22), see Zavari et al. [2012].

The weight $M_S$ should limit the peak of $S$ and is therefore chosen to be a constant. The peak of $G_{\mathbf{wu}}$ is also important to reduce in order to keep the control signal bounded, especially for high frequencies. A constant value of $W_{\mathbf{u}}$ is therefore also chosen. Finally, the weight $W_T$ is also chosen to be a constant for simplicity.

The system from $\mathbf{w}$ to the output includes an integrator, hence it is necessary to have at least two integrators in the open loop $GK$ in order to attenuate piecewise constant disturbances. The system $G$ has one integrator hence at least one integrator must be included in the controller. Including an integrator in the controller is the same as letting $|S(i\omega)| \to 0$, for $\omega \to 0$. Forcing $S$ to 0 is the same as letting $W_P$ approach $\infty$ when $\omega \to 0$. However, it is not possible to force pure integrators in the design since the generalised plant $P(s)$ is not possible to stabilise with marginally stable weights. Instead the pole is placed in the left half plane close to the origin. Zeros must be included in the design as well to get a proper inverse. The following weights have been proven to work

$$W_{\mathbf{u}} = 10^{-50/20}, \quad W_T = 10^{-8/20}, \tag{23a}$$

$$M_S = 10^{-8/20}, \quad W_P = \frac{(s+50)(s+15)(s+5)}{500(s+0.2)(s+0.001)^2}. \tag{23b}$$

The constant weights in the form $10^{-\lambda/20}$ can be interpret as a maximum value, for the corresponding transfer function, of $\lambda\,\text{dB}$.

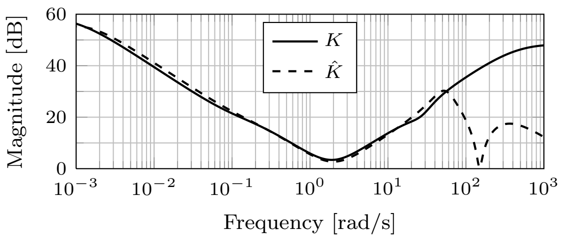


Fig. 3. Controller gains $|K|$ and $|\hat{K}|$.

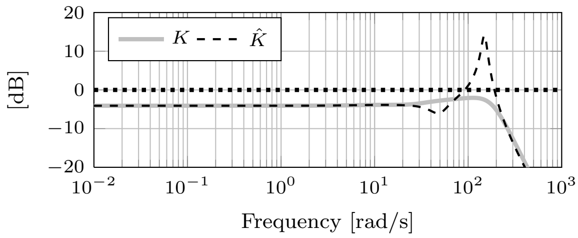


Fig. 4. Structured singular values for robust stability using the controllers $K$ and $\hat{K}$.

The augmented system $P$ is obtained using the command `augw(G,[Wp;MS],WU,WT)` in MATLAB, where $G$ is the system described by $\widetilde{\mathbf{A}}$, $\widetilde{\mathbf{B}}_u$, and $\widetilde{\mathbf{C}}$ in (18). The uncertainty description of $k(\delta)$ in (1) is used with $\alpha = 0.9167$, and $\beta = 0.5$, i.e., the nominal value is $k = k^{\text{high}}$, $\bar{k} = 83.33$, and $k(\delta) \in [16.67\ 183.33]$. The scaling parameter is chosen as $\kappa = 0.75$. Finally, the uncertainty model is updated according to

$$\mathbf{L} = \begin{pmatrix}\mathbf{0} & \widetilde{\mathbf{L}}^{\mathsf{T}}\end{pmatrix}^{\mathsf{T}}, \quad \mathbf{R} = \begin{pmatrix}\mathbf{0} & \widetilde{\mathbf{R}}\end{pmatrix} \tag{24}$$

where $\mathbf{0}$ is a zero matrix with suitable dimensions.

## 6. RESULTS

The optimisation problem in (14) is solved using Yalmip [Löfberg, 2004] and a controller $K$ of order $n_K = 6$ is obtained. A controller $\hat{K}$, with the same weights as for the robust stabilising controller $K$, using the optimisation problem in (14) without the LMI (14d) is derived to show the importance of the extra LMI for robust stability and also what is lost in terms of performance. The controller gains $|K|$ and $|\hat{K}|$ are shown in Figure 3, and they have a constant gain before $10^{-3}$ rad/s due to the pole at $s = -0.001$. The major difference is the notch for $\hat{K}$ around 100 rad/s and the high gain for $K$ for high frequencies.

The robust stability can be analysed using the structured singular value (SSV). The system is robustly stable if the SSV for the closed loop system from $\mathbf{w}_{\mathbf{\Delta}}$ to $\mathbf{z}_{\mathbf{\Delta}}$ with respect to the uncertainty $\mathbf{\Delta}$ is less than one for all frequencies. A thorough description of the SSV can be found in Skogestad and Postletwaite [2005]. Figure 4 shows the SSV for the closed loop system using $K$ and $\hat{K}$ and it can be seen that the SSV using $K$ is less than one (0 dB) for all frequencies whereas the SSV using $\hat{K}$ has a peak of approximately 15 dB. As a result $\hat{K}$ cannot stabilise the system for all perturbations, as expected.

The step responses for the controller $\hat{K}$ using the linearised system in $k = k^{\text{high}}$ and the controller $K$ using the linearised systems in $k = k^{\text{high}}$ and $k = k^{\text{low}}$ are shown

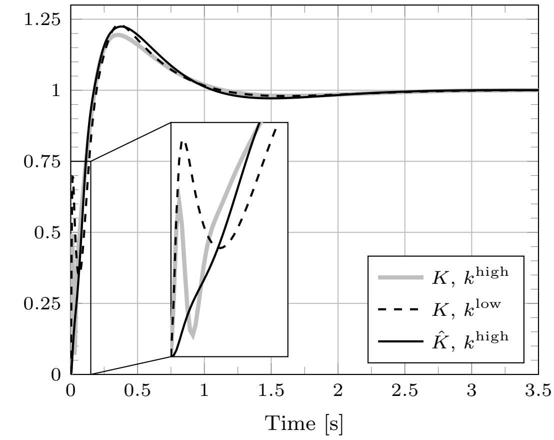


Fig. 5. Step response of the controllers $K$ and $\hat{K}$ using system linearised in $k^{\text{low}}$ and $k^{\text{high}}$. The first 0.15 s are magnified to show the initial transients.

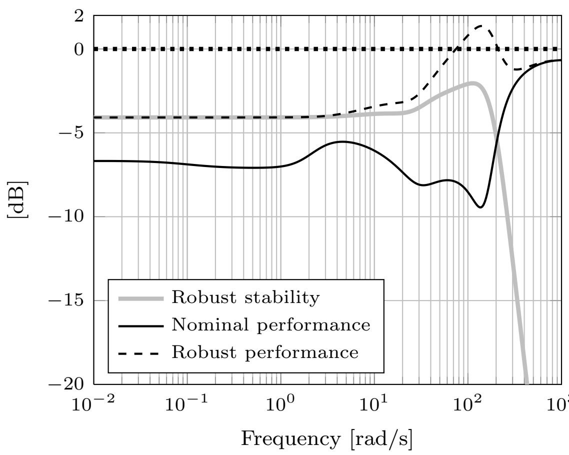


Fig. 6. Structured singular values for robust stability, nominal performance, and robust performance for the controller $K$.

in Figure 5. It can be seen that $\hat{K}$ is better than $K$ for the linearised system in the high stiffness region. It means that in order to get a controller that is robustly stable for $k(\delta)$, the performance has been impaired. It can also be seen that the performance for $K$ is better in the high stiffness region than in the low stiffness region, since the nominal value $k = k^{\text{high}}$.

The SSV can also be used for analysing nominal performance and robust performance, see Skogestad and Postletwaite [2005]. The requirement is that the SSV should be less than one for different systems with respect to some perturbations. Figure 6 shows the SSV for robust stability, nominal performance, and robust performance using $K$. It can be seen that the requirements for robust stability and nominal performance are satisfied. However, the requirement for robust performance is not satisfied. The reason is that the optimisation problem (14) does not take robust performance into account.

Finally, simulation of the non-linear model using $K$ is performed to show that the controller can handle dynamic changes in the stiffness parameter and not only stabilising the system for fixed values of the parameter. The non-linear model is simulated in Simulink using the disturbance signal in Figure 7(a), which is composed by steps and

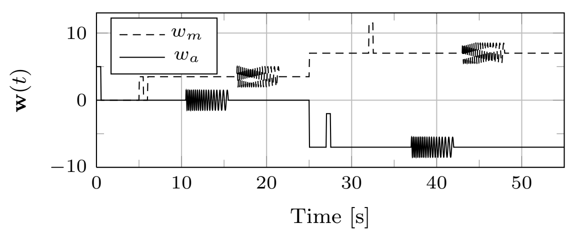


(a) Disturbance signal $\mathbf{w}(t)$ composed by steps and chirps.

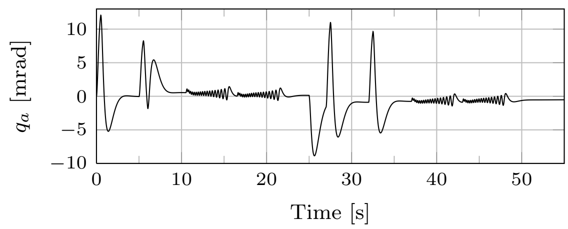


(b) Arm angle $q_a(t)$ expressed on the arm side of the gearbox.

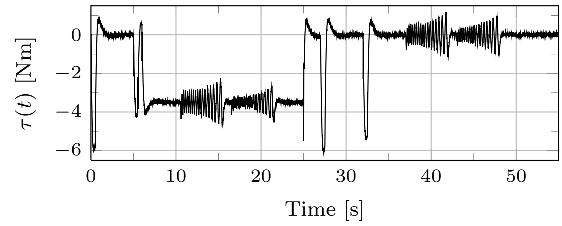


(c) Motor torque $\tau(t)$.

Fig. 7. Disturbance signal for the simulation experiment and the obtained arm angle and motor torque.

chirp signals. Figure 7(b) and 7(c) show the arm angle $q_a(t)$ on the arm side of the gearbox and the motor torque $\tau(t)$. From 0 s up to 25 s the system operates in the region $0 < |\Delta_q| < \Psi$ most of the time except for short periods of time when the step disturbances occur. The arm disturbance after 25 s keeps the system in the high stiffness region except for a few seconds in connection with the step disturbances.

The stationary error for $q_a(t)$ at the end is due to the fact that the controller only uses $q_m(t)$ and the constant $w_a(t)$ is not observable in $q_m(t)$ hence $q_a(t)$ cannot be controlled to zero. The primary position $q_m(t)$ does not have any stationary error.

## 7. CONCLUSIONS

A method to synthesise and design $\mathcal{H}_\infty$-controllers for flexible joints, with non-linear spring characteristics, is presented. The non-linear model is linearised in a specific operating point, where the performance requirements should be full filled. Moreover, an uncertainty description of the stiffness parameter is utilised to get robust stability for the non-linear system in all operating points. The resulting non-linear and non-convex optimisation problem can be rewritten as a convex, yet conservative, LMI problem using the Lyapunov shaping paradigm and a change of variables, and efficient solutions can be obtained using standard solvers.

Using the proposed synthesis method an $\mathcal{H}_\infty$-controller is computed for a specific model, where good performance can be achieved for high stiffness values while stability is achieved in the complete range of the stiffness parameter. A controller derived with the same performance requirement but without the additional stability constraint is included for comparison. By analysing the structured singular values for robust stability for the two controllers it becomes clear that the controller without the extra stability constraint will not be stable for the parameter variations introduced by the non-linear stiffness parameter.

In the synthesis method it is assumed that the parameter $\delta$ changes arbitrarily fast, which is a conservative assumption for real systems. It would therefore be a good idea to have a limited change in $\delta$ in the future development of the method. Moreover, the use of a common Lyapunov matrix $\boldsymbol{\mathcal{P}}$ must be relaxed to reduce the conservatism further. Here, the path following method from Hassibi et al. [1999], Ostertag [2008] can be further investigated.

## REFERENCES

P. Axelsson, R. Karlsson, and M. Norrlöf. Bayesian state estimation of a flexible industrial robot. *Contr. Eng. Pract.*, 20(11):1220–1228, November 2012.

W. Chen and M. Tomizuka. Direct joint space state estimation in robots with multiple elastic joints. *IEEE/ASME Trans. Mechatron.*, 2013. DOI: 10.1109/TMECH.2013.2255308.

P. Gahinet and P. Apkarian. A linear matrix inequality approach to $\mathcal{H}_\infty$ control. *Int. J. of Robust and Nonlin. Contr.*, 4(1):421–448, 1994.

A. Hassibi, J. How, and S. Boyd. A path-following method for solving BMI problems in control. In *Proc. of the American Contr. Conf.*, pages 1385–1389, San Diego, CA, USA, June 1999.

J. Löfberg. YALMIP: A toolbox for modeling and optimization in MATLAB. In *Proc. of the IEEE Int. Symp. on Comp. Aided Contr. Syst. Design*, pages 248–289, Taipei, Taiwan, September 2004. URL http://users.isy.liu.se/johanl/yalmip.

A. Megretski and A. Rantzer. System analysis via integral quadratic constraints. *IEEE Trans. Automat. Contr.*, 42(6):819–830, June 1997.

E. Ostertag. An improved path-following method for mixed $\mathcal{H}_2/\mathcal{H}_\infty$ controller design. *IEEE Trans. Automat. Contr.*, 53(8):1967–1971, September 2008.

M. Ruderman and T. Bertram. Modeling and observation of hysteresis lost motion in elastic robot joints. In *Proc. of the 10th Int. IFAC Symp. on Robot Contr.*, pages 13–18, Dubrovnik, Croatia, September 2012.

H. G. Sage, M. F. de Mathelin, and E. Ostertag. Robust control of robot manipulators: A survey. *Int. J. of Contr.*, 72(16):1498–1522, 1999.

C. Scherer. LMI relaxations in robust control. *Euro. J. of Contr.*, 12(1):3–29, 2006.

C. Scherer, P. Gahinet, and M. Chilali. Multiobjective output-feedback control via LMI optimization. *IEEE Trans. Automat. Contr.*, 42(7):896–911, July 1997.

S. Skogestad and I. Postletwaite. *Multivariable Feedback Control, Analysis and Design.* John Wiley & Sons, Chichester, West Sussex, England, second edition, 2005.

`mixedHinfsyn`. MATLAB-software, 2013. Available at http://www.kuleuven.be/optec/software/mixedhinfsyn.

T. Tjahjowidodo, F. Al-Bender, and H. Van Brussel. Nonlinear modelling and identification of torsional behaviour in harmonic drives. In *Proc. of the Int. Conf. on Noise and Vibration Engineering*, pages 2785–2796, Leuven, Belgium, September 2006.

T. D. Tuttle and W. P. Seering. A nonlinear model of a harmonic drive gear transmission. *IEEE Trans. Robot. Automat.*, 12(3): 368–374, June 1996.

K. Zavari, G. Pipeleers, and J. Swevers. Multi-$\mathcal{H}_\infty$ controller design and illustration on an overhead crane. In *Proc. of the IEEE Conf. on Contr. App.. Part of the IEEE Multi-Conf. on Syst. and Contr.*, pages 670–674, Dubrovnik, Croatia, October 2012.

K. Zhou, J. C. Doyle, and K. Glover. *Robust and Optimal Control.* Prentice Hall Inc., Upper Saddle River, NJ, USA, 1996.